Magnetic circular dichroism in $4d \rightarrow 4f$ resonant photoemission and photoabsorption of Gd metal

K. Starke
Institut für Experimentalphysik, Freie Universität Berlin, Arnimallee 14, D-14195 Berlin-Dahlem, Germany and AT&T Bell Laboratories, Murray Hill, New Jersey 07974

E. Navas, E. Arenholz, Z. Hu, and L. Baumgarten*
Institut für Experimentalphysik, Freie Universität Berlin, Arnimallee 14, D-14195 Berlin-Dahlem, Germany

G. van der Laan
Daresbury Laboratory, Warrington WA4 4AD, United Kingdom

C. T. Chen†
AT&T Bell Laboratories, Murray Hill, New Jersey 07974

G. Kaindl
Institut für Experimentalphysik, Freie Universität Berlin, Arnimallee 14, D-14195 Berlin-Dahlem, Germany
(Received 9 August 1996)

A consistent description of magnetic circular dichroism (MCD) in resonant $4d \rightarrow 4f$ photoemission (PE) and $4d$ photoabsorption (PA) from magnetized rare-earth metals is presented. In the case of ferromagnetic Gd metal it is found that the MCD of the resonant $4f$PE spectra varies strongly when the photon energy is scanned across the resonance region. We show that the spectral shape of the $4f$PE multiplet is determined by the total angular momentum of the intermediate $4d^9 4f^8$ PA state, which is reflected in the sign of the PA-MCD at the excitation energy. [S0163-1829(97)10404-0]

Photoabsorption (PA) and photoemission (PE) from magnetically ordered materials using circularly polarized x rays — known as magnetic-circular-dichroism (MCD) spectroscopies — are relatively new additions to the analytical toolbox of magnetism, attracting considerable interest both from experimental[1–4] and theoretical points of view.[5,6] MCD in PA has been widely used at transition-metal $L_{2,3}$ edges, where it allows an element-specific analysis of heteromagnetic systems and multilayers.[7] In PE, particularly large MCD effects have been observed for the $4f$ multiplets of rare earths,[4,8] which can be readily understood within atomic-multiplet theory considering dipole-selection rules for excitation with circularly polarized light.

When applied to multicomponent systems, like thin-film compound magnets or magnetic interfaces, it is often desirable to enhance selectively the cross section of an individual element by resonant PE, e.g., using the $4d \rightarrow 4f$ giant-resonance region of the rare earths.[9] Resonant PE is caused by a coherent superposition of the direct PE channel, $4f^n \rightarrow 4f^{n-1} \varepsilon l$, and the indirect channel $4f^n \rightarrow 4d^9 4f^{n+1} \rightarrow 4f^{n-1} \varepsilon l$, where the $4d$-hole state couples to the PE final state via autoionization.[9,10] The strong $4d$-$4f$ overlap in rare earths gives rise to large correlation energies, and hence to widely split $4d^9 4f^{n+1}$ multiplets of intermediate PA states with different angular momenta (L', S', J'). Gd has a typical $4d$-PA spectrum consisting of a broad and dominant absorption peak (giant resonance), preceded by narrow and weak lines (pre-edge region). First theoretical[11] and experimental[12] studies have revealed sizeable PA-MCD effects in both regions.

In this communication, we report a study of MCD in resonant PE, using Gd metal as an example. When the photon energy is changed across the Gd $4d \rightarrow 4f$ excitation region, the PE-MCD spectrum varies substantially. Based on atomic-multiplet theory, we present a consistent picture of MCD in resonant $4d \rightarrow 4f$PE and in $4d \rightarrow 4f$PA, where the spectral changes can be explained by the angular momentum of the $4d^9 4f^{n+1}$ intermediate state. The resonant PE-MCD spectrum, taken at a particular photon energy, was found to be correlated with the sign of the PA-MCD signal at that energy. Furthermore, we found a natural explanation for the widely different widths of the PA lines in the giant-resonance and pre-edge regions, based on super-Coster-Kronig (sCK) decay rates of the $4d$-core-excited intermediate states.

The PE experiments were performed with circularly polarized light from the SX-700/III beamline at the Berliner Elektronenspeicherring für Synchrotronstrahlung delivering $\cong 75\%$ circularly polarized light ($S_3 \cong 0.75$).[13] Epitaxial Gd(0001) metal films, (110 ± 20) Å thick, were prepared by vapor deposition onto a W(110) substrate at room temperature. Subsequent annealing for 5 min at 800 K resulted in well-ordered, low-coercivity Gd films. During deposition, the pressure remained below 10^{-10} mbar, returning to the base pressure of 2×10^{-11} mbar within seconds. Chemical cleanness was controlled by looking for O-1s and C-1s PE signals, which were both below the limit of detection of a few percent of a monolayer. The Gd film was magnetized remanently in plane by field pulses from a closeby solenoid, checked *in situ* via the magneto-optical Kerr effect. To achieve large MCD effects, a grazing-incidence geometry (15°) was chosen for the incoming light, and photoelectrons were collected along the surface normal by a hemispherical analyzer with an energy resolution of $\cong 90$ meV full width at half maximum and acceptance cone of $\pm 5°$. The PA spectra

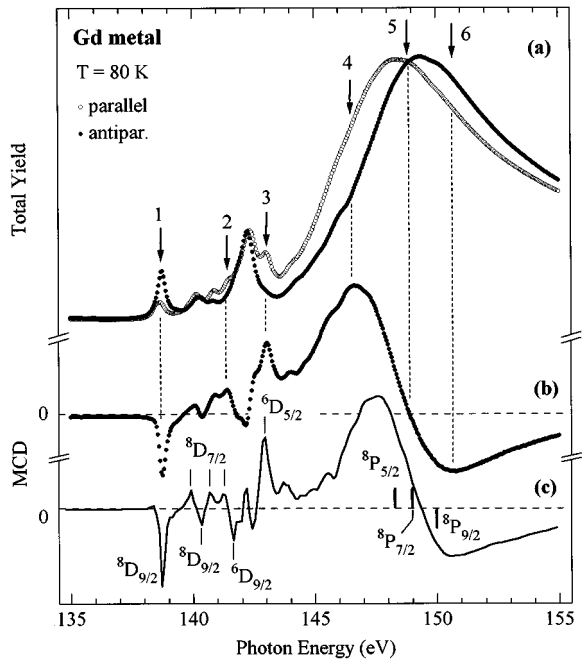

FIG. 1. (a) Photoabsorption spectra in the Gd $4d \rightarrow 4f$ excitation region, for parallel (open dots) and antiparallel (filled dots) orientation of photon spin and sample magnetization. (b) Experimental and (c) calculated PA-MCD spectra.

were recorded in total-electron-yield mode using circularly polarized light ($S_3 \cong 0.85$) from the Dragon beamline at the National Synchrotron Light Source,[14] operated with an energy resolution of $\cong 90$ meV, well below the intrinsic widths of the narrow preedge lines of the Gd-4*d* PA spectrum.

Theoretical MCD spectra in PA and PE were calculated in intermediate coupling with Cowans's computer code,[15] using the relativistic Hartree-Fock plus statistical-exchange method. To include intra-atomic correlation effects, the Coulomb and exchange integrals were reduced to 80%, and the sCK matrix elements R to 66% of the atomic values.[16] For calculation of the PA spectra, radiative transitions were taken into account to first order as well as the sCK transitions $4d^9 4f^8 \rightarrow 4d^{10} 4f^6 + \varepsilon l$ to infinite order.[17] For resonant PE, transitions to continuum states with parity-allowed angular momenta up to $\ell = 8$ were considered. Line broadening by the photoelectron final state as well as experimental resolution was included by convolution with a Lorentzian of $\Gamma = 0.18$ eV and a Gaussian of $\sigma = 0.085$ eV.

Figure 1(a) displays high-resolution 4*d* PA spectra from Gd metal at 80 K, for parallel and antiparallel orientations of magnetization and photon spin. Upon magnetization reversal, the giant-resonance peak shifts by $\cong 1$ eV, and the line intensities in the preedge region change drastically, as observed previously by Muto *et al.*[12] The PA-MCD spectrum, obtained as the difference of both PA spectra, is given in (b), and the calculated spectrum, corrected for saturation,[18] in (c). The most pronounced features have been labeled according to their leading-term contribution.

In the limit of vanishing 4*d* spin-orbit (s.o.) coupling, only $^8P_{J'}$ states ($J' = 5/2$, 7/2, and 9/2) would be dipole-excited from the $^8S_{7/2}$ ground state of Gd (with $\Delta L = +1$), giving rise to the giant-resonance peaks [thick vertical bars in Fig. 1(c)]. 4*d* s.o. coupling leaves only $\Delta J = \pm 1$, 0 as a strict selection rule, allowing additional transitions to $^8D_{J'}, ^6D_{J'} \ldots$ states in the pre-edge region. The calculated energies of the low-spin sextet states ($S = 5/2$) agree well with earlier results.[9]

TABLE I. Intensities of $\Delta M = \pm 1$ transitions from the $|J = 7/2, M = -7/2\rangle$ ground state to intermediate states J'; the difference provides the PA-MCD.

J'	$\Delta M = +1$	$\Delta M = -1$	PA-MCD
5/2	3/4	0	3/4
7/2	2/9	0	2/9
9/2	1/36	1	−35/36

The good signal-to-noise ratio and the high resolution of the PA-MCD spectrum (about four times better than the smallest intrinsic width of $\cong 350$ meV) allow a detailed comparison with theory. Hereby, a unique property of the PA-MCD spectrum, not reported before, becomes obvious: states with dominant angular momentum $J' = 9/2$ give rise to minima, while those with $J' = 5/2$ and — though less pronounced — $J' = 7/2$ lead to maxima. This correlation follows from the dipole-selection rule $\triangle M = \pm 1$ for excitation with circularly polarized light. As shown in Table I, transitions with $\Delta J = -\Delta M$ dominate the PA spectra, i.e., starting from the fully magnetized ground state of Gd $|J = 7/2, M = -7/2\rangle$, only PA states with $J' = 9/2$ are reached for antiparallel orientation, $\Delta M = -1$; for parallel orientation, $\Delta M = +1$, predominantly $J' = 5/2$ and 7/2 states are reached. The overall agreement between experiment and theory is striking, supporting the assignment of the total angular-momentum character of the main peaks. Our theoretical analysis of the Gd-4*d* PA spectrum includes a coupling of the $4d^9 4f^8$ states to the $4f^6 \varepsilon \ell$ continuum via sCK decay; in the pre-edge region, the sCK decay rate is roughly two orders of magnitude smaller than for the giant-resonance ^8P states.[16] This provides a simple explanation of the separation of the Gd-4*d*PA spectrum into narrow and broad peaks.

Having identified the total angular-momentum J' of the Gd-4*d*PA states, which serve as intermediate states for the indirect channel in resonant PE, we now turn to the key issue of the present paper, namely, MCD in resonant $4d \rightarrow 4f$PE. The MCD spectrum of the off-resonance Gd$4f^6\, ^7F_{J''}$($J'' = 0, \ldots 6$) PE multiplet, shown in Fig. 2(a), has been analyzed extensively.[4,6,8] For antiparallel orientation of sample magnetization and photon spin ($\Delta M = -1$), transitions via $J' = 9/2$ states prevail, resulting in a maximum at low J'' values, i.e., a $^7F_{J''}$ PE multiplet with a rounded shape; for parallel orientation ($\Delta M = +1$), the multiplet peaks on the high-binding-energy side. In Fig. 2(b), pairs of *resonant* 4*f* PE spectra are shown for various photon energies in the $4d \rightarrow 4f$ region. For both orientations, the shape of the PE multiplet changes considerably with excitation energy.

A qualitative picture of resonant PE-MCD is reached in the following way: By tuning to a specific PA line, e.g., to line 1 in Fig. 1 with dominant $J' = 9/2$ character, the $^7F_{J''}$ multiplet, populated by indirect resonant PE, will assume a rounded shape, though to a different extent for parallel and antiparallel orientations, since the excitation probability to the $J' = 9/2$ state differs appreciably for $\Delta M = +1$ and $\Delta M = -1$ (see Table I). By tuning to a PA line with $J' = 5/2$ (e.g., energy 3 in Fig. 1), one analogously expects a shift of the

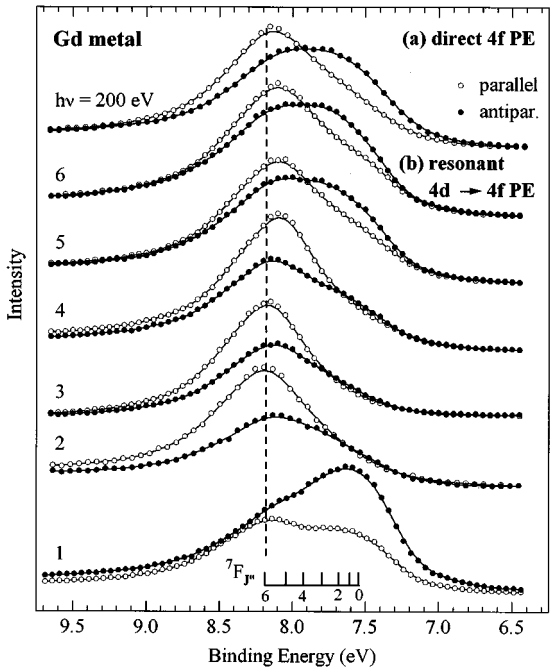

FIG. 2. (a) Off-resonance PE spectra of the Gd $4f^6\ ^7F_{J''}$ multiplet for parallel (open dots) and antiparallel (filled dots) orientations of photon spin and sample magnetization. The bar diagram (bottom) gives the J'' multiplet. (b) Resonant PE spectra for various photon energies across the $4d \rightarrow 4f$ excitation region; the numbers refer to photon energies marked by vertical arrows in Fig. 1.

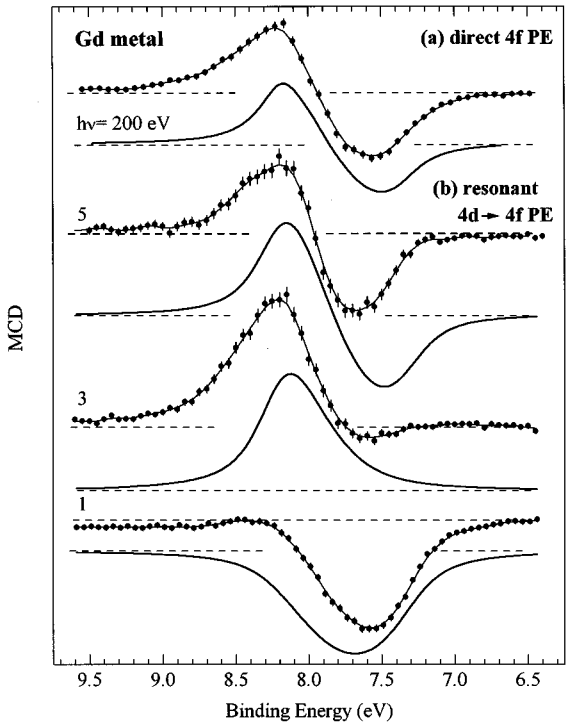

FIG. 3. Comparison of experimental (dots) and calculated (drawn lines) PE-MCD spectra: (a) off-resonance, (b) on-resonance; the numbers refer to photon energies marked by vertical arrows in Fig. 1.

PE-multiplet maximum to high-J'' values. In the giant-resonance region, except for energy 4, the changes will be less pronounced because the broad PA states overlap strongly. This simplified picture accounts for the observed spectral changes, but neglects the additional possibility of a coupling of the angular momenta of the photoelectron and the PE final state, which opens up through $4d$ s.o. interaction, particularly in the pre-edge region.

For a quantitative analysis of the resonant PE spectra, the matrix element for angle-integrated PE in the indirect channel, $LSJM \rightarrow L'S'J' \rightarrow (L''S''J'')\ (\not{\ell} sj)$, is given as

$$\langle LSJM|P^1_\Delta|(L''S''J'')(\not{\ell} sj)L'S'J'\rangle$$

$$\propto (2J'+1)^{1/2}\begin{pmatrix} J & 1 & J' \\ -M & -\Delta M & M+\Delta M \end{pmatrix} \times \sum_J (2j+1)\begin{Bmatrix} S'' & L'' & J'' \\ s & \not{\ell} & j \\ S' & L' & J' \end{Bmatrix}^2 .$$

The $3j$ symbol (in parentheses) describes the ΔM dependence of the absorption process; the squares of the $3j$ symbols, multiplied by the multiplicities $(2J'+1)$, are given in Table I. The shape of the resonant-PE spectrum (relative intensities of J'' components) is determined by the squared $9j$ symbol (in curly braces), which describes the recoupling of the momenta of the intermediate state $(S'L'J')$, the PE final state $(S''L''J'')$, and the outgoing photoelectron $(s\not{\ell} j)$, where $g(\not{\ell}=4)$ is the dominant PE decay channel.[16] The shape of the resonant PE spectrum will be different for each $L'S'J'$ state ($^8D, ^6D, ^8P, \ldots$). We find, however, that the spectra depend primarily on J' and less on L' and S'. Figure 3(b) provides a comparison of the experimental and calculated resonant MCD-PE spectra, with the off-resonance case presented in (a). When tuning the photon energy from energy 1 to energy 3, the PE-MCD spectrum changes from negative to positive, and shifts from the low-J'' to the high-J'' region. The excellent agreement between experiment and theory in the preedge region supports our picture of a selective resonance enhancement of specific PE excitation channels by tuning to a PA state with a specific J'.

At resonance energy 5, where the PA-MCD signal vanishes, the PE-MCD spectrum resembles the off-resonance case closely. Here the intermediate states are mainly $L'=1$ and $J'=5/2$ and 7/2. The shape of the resonant PE spectrum, comprising all three J'' distributions according to the $3j$ symbols, will be the same as in direct PE, if the polarization of the core-excited state averages out.[19] Such a situation occurs approximately in the center of the giant resonance peak at energy 5, where the MCD signal in PA vanishes due to the broad overlapping ^8P PA lines.

In conclusion, a consistent description of the Gd-$4d$ PA spectrum has been presented, including an identification of the angular-momentum character and an explanation of the strongly different lifetime widths of the main PA lines. The close agreement between the $4d$-$4f$ resonant PE-MCD spectra and the results of atomic-multiplet calculations supports the approximate validity of the simple picture presented for resonant $4d \rightarrow 4f$PE: Tuning to a specific line of the $4d$-PA spectrum leads to a selective enhancement of PE multiplet components, governed by the total angular momentum of the intermediate PA state. The PE-MCD spectrum at giant resonance closely resembles the off-resonance spectrum, when

the PA-MCD vanishes at the selected photon energy. Thus the strongly enhanced $4d$-$4f$ resonant PE opens perspectives in applications of PE-MCD to element-specific analysis of thin multicomponent magnetic systems, as well as to domain imaging by PE microscopy.[20]

Supported by the Bundesminister für Bildung, Wissenschaft, Forschung und Technologie, Project No. 05-621-KEB 8, and the SfB-290/TPA6 of the Deutsche Forschungsgemeinschaft; K.S. would like to thank the latter for financial support, and Bell Laboratories for hospitality.

*Present address: Forschungszentrum Jülich, D-52425 Jülich, Germany.

†Present address: Synchrotron-Radiation Research Center, Hsinchu 300, Taiwan.

[1] G. Schütz *et al.*, Phys. Rev. Lett. **58**, 737 (1987).

[2] C. T. Chen *et al.*, Phys. Rev. B **42**, 726 (1990).

[3] L. Baumgarten *et al.*, Phys. Rev. Lett. **65**, 492 (1990).

[4] K. Starke *et al.*, Phys. Rev. B **48**, 1329 (1993).

[5] B. T. Thole *et al.*, Phys. Rev. Lett. **68**, 1943 (1992), and references therein.

[6] G. van der Laan and B. T. Thole, Phys. Rev. B **48**, 210 (1993), and references therein.

[7] See, e.g., M. G. Samant *et al.*, Phys. Rev. Lett. **72**, 1112 (1994).

[8] E. Arenholz *et al.*, Phys. Rev. B **51**, 8211 (1995).

[9] F. Gerken, J. Barth, and C. Kunz, Phys. Rev. Lett. **47**, 993 (1981).

[10] *Giant Resonances in Atoms, Molecules and Solids*, edited by J. P. Connerade *et al.* (Plenum, New York, 1987).

[11] S. Imada and T. Jo, J. Phys. Soc. Jpn. **59**, 3358 (1990).

[12] S. Muto *et al.*, J. Phys. Soc. Jpn. **63**, 1179 (1994).

[14] H. Petersen *et al.*, Nucl. Instrum. Methods Phys. Res. Sect. A **333**, 594 (1993).

[15] C. T. Chen, Rev. Sci. Instrum. **63**, 1229 (1992).

[16] R. D. Cowan, *The Theory of Atomic Structure and Spectra* (University of California Press, Berkeley, 1981).

[17] Atomic Hartree-Fock values of the Slater integrals and spin-orbit parameters of Gd are given in G. van der Laan *et al.*, Phys. Rev. B **53**, R 5998 (1996). The unscaled sCK matrix elements are: $R(4d,4f;4f,\varepsilon s) = -0.2935$ eV/$\sqrt{\text{Ry}}$; $R^k(4d,4f;4f,\varepsilon d) = -0.0253$, 0.0278, and 0.0428 eV/$\sqrt{\text{Ry}}$; and $R^k(4d,4f;4f,\varepsilon g) = -3.3500$, -1.9033, and -1.2807 eV/$\sqrt{\text{Ry}}$. The dipole-matrix elements are $\langle 4d\|r\|4f\rangle = 1.1163$ a.u., $\langle 4f\|r\|\varepsilon d\rangle = 0.039\,15$ a.u./$\sqrt{\text{Ry}}$; and $\langle 4f\|r\|\varepsilon g\rangle = -0.345\,25$ a.u./$\sqrt{\text{Ry}}$.

[18] H. Ogasawara *et al.*, Solid State Commun. **81**, –645 (1992).

[19] B. T. Thole *et al.*, Phys. Rev. B **32**, 5107 (1985).

[20] G. van der Laan and B. T. Thole, J. Phys. Condens. Matter **7**, 9947 (1995).

[21] T. Kachel, W. Gudat, and K. Holldack, Appl. Phys. Lett. **64**, 655 (1994).